Contents

THERMO–MECHANICAL CONTACT IN CASTING ANALYSIS

Chiumenti, M.

International Center for Numerical Methods in Engineering, Edifici C1, Campus Nord, Polytechnic University of Catalonia, 08034 Barcelona, Spain
chiument@cimne.upc.edu

1 Introduction

The aim of this study is to show the intrinsic difficulties involved and the strategy adopted in simulating a *foundry process*. Figure 1 shows the filling evolution, that is, the position of the metal front at different time–steps in a numerical simulation of a high–pressure die–casting process. The following phases of the process are solidification, cooling of the part and, finally, opening of the mould.

Up to now, most of the simulations have been purely thermal to study the evolution of the solidification and cooling phenomena. This is mainly due to the fact that this strategy is easier and less costly and therefore more convenient for large–scale industrial simulations.

On the other hand, the *fully coupled thermo–mechanical analysis* is the natural framework to represent the heat flow exchange, both the final shape of the casting part, and the evolution of the residual stresses induced by the manufacturing operations. Accurate modelling of both stresses and deformations of the part during the solidification and the cooling phases is crucial to capture the thermal pattern (temperature and solidification evolution) in aluminium casting or, more generally, when a permanent mould is used. In fact, the thermal deformation of both part and mould modifies the original interfacial heat transfer among all the casting tools involved in the process. The relationship between the heat transfer coefficient and mechanical quantities, such as the open air–gap or the contact pressure, has been experimentally proven. Hence, the mechanical analysis coupled with the thermal simulation is required to produce a reliable casting numerical model.

More specifically, this chapter will focus on the description of the *thermo–mechanical contact model* model necessary to study the interaction among all the casting tools during the solidification and cooling processes. This is possibly the key point in a casting simulation, as it plays an extremely important role an coupling the thermo–mechanical problem in both ways.

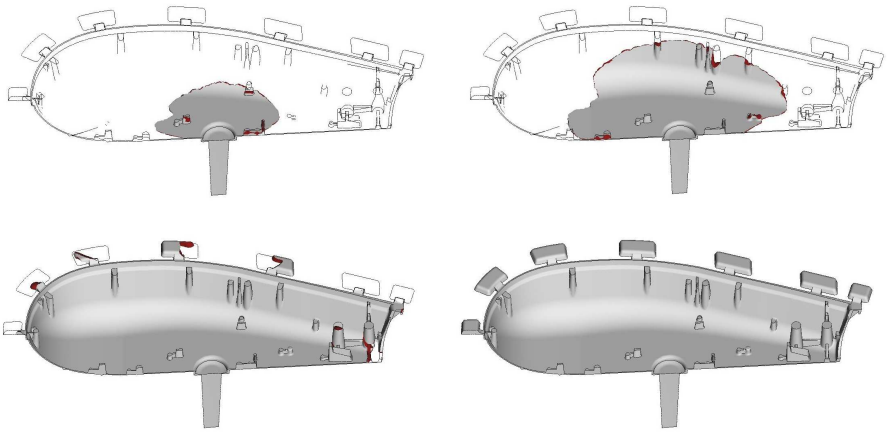

Fig. 1. Filling evolution in a HP Die–casting process

2 Governing Equations

The system of partial differential equations governing the coupled thermo–mechanical problem is defined by the momentum and energy balance equations, restricted by the inequalities arising from the second law of thermodynamics. This system must be supplemented with suitable constitutive equations and prescribed boundary and initial conditions.

2.1 Strong Form of the Governing Equations

Let Ω be the domain with smooth boundary $\partial\Omega$ of a continuum body β. Let $[0,T]$ be the time interval of interest. The strong form of the balance of momentum equation, also known as Cauchy's equation of motion, is given by:

$$\nabla \cdot \sigma + \mathbf{b} = \rho_0 \frac{d\mathbf{v}}{dt}$$

where σ is the Cauchy's stress tensor, $\mathbf{b}$ is the vector of forces per unit volume, ρ_0 is the density in the reference configuration and $\mathbf{v}$ is the velocity field.

The balance of energy equation can be written as:

$$\dot{E} = \sigma : \dot{\varepsilon} + \dot{Q}$$

so that the increase of the internal energy $\dot{E}$ per unit volume consists of two parts: the stress power $\sigma : \dot{\varepsilon}$, which represents the mechanical work done by the external forces not converted into kinetic energy, and the heat supplied to the system $\dot{Q} = \dot{R} - \nabla \cdot \mathbf{Q}$ in terms of internal sources per unit volume and heat flow through the boundary, $\dot{R}$ and $-\nabla \cdot Q$, respectively. The balance of energy equation is the strong form for the First Law of Thermodynamics.

On the other hand,the Second Law of Thermodynamics limits the direction of the energy transformations and postulates that there exists a state function called enthalpy H such that

$$\dot{H} = \dot{Q} + \dot{D}$$

where $\dot{D} \geq 0$ is a thermo–mechanical variable usually referred to as thermo–mechanical dissipation and represents the energy dissipated (transformed in heat) in case of irreversible process. The above equation is known in the literature as the Clausius–Plank equation. It is an energy balance equation accounting for reversible and irreversible (dissipated) heat flow, $\dot{Q}$ and $\dot{D}$, respectively.

Thus, the first order system of equations that governs the coupled thermo–mechanical problem can be stated as follows (see Agelet de Saracibar, C. et al. [2001], Agelet de Saracibar, C. et al. [1999b], Agelet de Saracibar, C. et al. [1999a] and Chiumenti, M. et al. [1999]):

$$\begin{aligned} \dot{\mathbf{u}} &= \mathbf{v} \\ \rho_0 \dot{\mathbf{v}} &= \nabla \cdot \sigma + \mathbf{b} \\ \dot{H} &= \dot{R} - \nabla \cdot Q + \dot{D} \end{aligned}$$

2.2 Weak Form of the Balance of Momentum Equation

First of all, it must be pointed out that to represent the liquid–like metal behaviour correctly the volumetric incompressibility should be taken into account during the solidification process. The same requirement is necessary during the cooling phase. In fact, a J2–thermo–elasto–visco–plastic constitutive model (fully deviatoric) is generally adopted, leading to an isochoric evolution of the deformations. As a result, a suitable strategy must be chosen to deal with this constraint. Many techniques have been proposed to solve this problem when quadrilateral or hexahedral elements are used: Q1P0 formulation or *enhanced* element technologies. However, when linear tetrahedral elements are selected (as is necessary for complex industrial geometries), a convenient approach to deal with the incompressibility behaviour assumes as starting point the mixed $\mathbf{u}/p$ formulation of the balance of momentum equation, where the driving variables are both displacements and pressure fields, $\mathbf{u}$ and p, respectively:

$$\nabla \cdot \mathbf{s} + \nabla p + \mathbf{b} = \rho_0 \frac{d\mathbf{v}}{dt}$$

where $\mathbf{s}$ is the deviatoric part of the Cauchy's stress tensor, defined as $\sigma = p\mathbf{1} + \mathbf{s}$.

Let $\delta\eta$ and δq be the test functions associated to the displacement and pressure fields $\mathbf{u}$ and p, respectively. The weak form of the balance of momentum equation in the hypothesis of a quasi–static process can be expressed in the mixed format as:

$$\int_\Omega \delta\eta^T \left(\nabla\cdot\mathbf{s}+\nabla p\right) dV + \int_\Omega \left(\delta\eta^T\mathbf{b}\right) dV = 0$$
$$\int_\Omega \delta q^T \left(\nabla\cdot\mathbf{u}+\frac{p}{K}-e^\theta\right) dV = 0$$

where K is the compressibility modulus (bulk modulus) and e^θ is the thermal (volumetric) deformation. Applying the divergence theorem to the first equation yields:

$$\int_\Omega \left(\nabla^S\delta\eta^T\mathbf{s}\right) dV + \int_\Omega \left(\nabla\cdot\eta^T p\right) dV =$$
$$\int_\Omega \left(\delta\eta^T\mathbf{b}\right) dS + \int_{\partial\Omega} \left(\delta\eta^T\overline{\mathbf{t}}\right) dS + \int_{\partial\Omega} \left(\delta\eta^T\mathbf{t}_c\right) dS$$

where $\overline{\mathbf{t}} = \sigma\cdot\mathbf{n}$ is the prescribed surface traction while $\mathbf{t}_c$ is the contact pressure due to contact interaction.

Observe that in case of liquid–like behaviour, $K\rightarrow\infty$ and e^θ, so that the continuity equation transforms into:

$$\int_\Omega \left(\delta q^T\nabla\cdot\mathbf{u}\right) dV = 0$$

and a stabilisation technique is necessary to ensure stability when linear elements are used. It can be proven that neither standard P1 nor P1/P1 mixed elements pass the Babuska–Brezzi stability condition, Brezzi, F. and Fortin, M. [1991]. An attractive alternative to circumvent this condition can be achieved by introducing a stabilizing term in the continuity equation.

A first possibility is the so–called Galerkin Least–Squares (GLS) method, which introduces a stabilisation term in the form

$$\int_\Omega \left(\delta q^T\nabla\cdot\mathbf{u}\right) dV = \sum_{e=1}^{Nelem} \tau_e \int_\Omega \left(\nabla q^T\nabla p\right) dV$$

that is, an element–by–element stabilisation term based on the residual of the balance of momentum equation.

Another possibility is the Orthogonal Sub–Grid Scale (OSGS) approach Agelet de Saracibar, C. et al. [2006], Agelet de Saracibar, C. et al. [2003], Agelet de Saracibar, C. et al. [2002a], Agelet de Saracibar, C. et al. [2002b], Codina, R. [2000] where the resulting stabilizing term is added as

$$\int_\Omega \left(\delta q^T\nabla\cdot\mathbf{u}\right) dV = \sum_{e=1}^{Nelem} \tau_e \int_\Omega \left[\nabla q^T\left(\nabla p-\pi\right)\right] dV$$

where π is the smoothed projection of the pressure gradient computed at each time step as

$$\int_{\Omega} \left[\nabla\omega^{T}\left(\nabla p - \pi\right)\right] dV = 0$$

π being the test functions associated to the pressure gradient field.

The stabilisation coefficient τ_e introduced in the continuity equation is usually expressed in the form: $\tau_e = h_e c/2G$, where h_e is the characteristic element length, G is the shear modulus of the material and c is a constant obtained through numerical testing.

Observe that the OSGS method introduces a smaller stabilisation term to relax the incompressibility condition, resulting in a less diffusive and more precise algorithm than the GLS method. However, OSGS is more expensive from the computational point of view, especially for commercial application. The smooth projection of the pressure gradient, π, is an extra nodal variable to be computed and stored.

2.3 Weak Form of the Balance of Energy Equation

Let $\delta\vartheta$ be the test function associated with the temperature field T. The weak form of the balance of energy equation reads:

$$\int_{\Omega} \left(\delta\vartheta\dot{H}\right) dV = \int_{\Omega} \left(\delta\vartheta\dot{R}\right) dV - \int_{\Omega} \left(\delta\vartheta\nabla\cdot Q\right) dV + \int_{\Omega} \left(\delta\vartheta\dot{D}\right) dV$$

Integrating by parts, the above equation can be rewritten as follows:

$$\int_{\Omega} \left(\delta\vartheta\dot{H}\right) dV + \int_{\Omega} \left[\nabla\left(\delta\vartheta\right) k\nabla T\right] dV = G^{\theta}$$

G^{θ} being the thermal work due to the internal sources, mechanical dissipation and heat flux through the boundaries

$$G^{\theta} = \int_{\Omega} \left(\delta\vartheta\dot{R}\right) dV + \int_{\Omega} \left(\delta\vartheta\dot{D}\right) dV + \int_{\partial\Omega} \left(\delta\vartheta\overline{q}\right) dS + \int_{\partial\Omega} \left(\delta\vartheta Q_c\right) dS$$

where $\overline{q} = \mathbf{Q}\cdot\mathbf{n}$ is the prescribed heat flux through to the boundaries and Q_c is the heat flux due to thermal contact interaction.

3 Geometry and FE Mesh

Once the equations to be solved are defined, the main difficulty to be taken into account when modelling a casting process is the geometrical definition of all casting tools involved in the manufacturing process. The complexity of such geometries makes the meshing operation very difficult. Figure 2 shows the intricacy of the sand casting system used to manufacture excavator teeth.

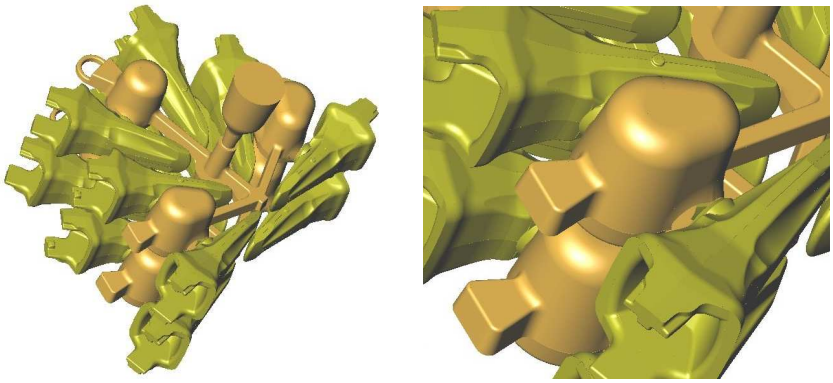

Fig. 2. Sand gravity casting. CAD geometry of the foundry system.

The high number of casting tools involved in the simulation such as part, moulds, cores, cooling channels, chillers, etc... requires an important CAD effort which leads to much greater meshing problems. Figure 3 shows the steel mould used in a gravity die–casting process and the corresponding casting part (carter). It is possible to distinguish the feeding system, the cooling system, and the cores positioning.

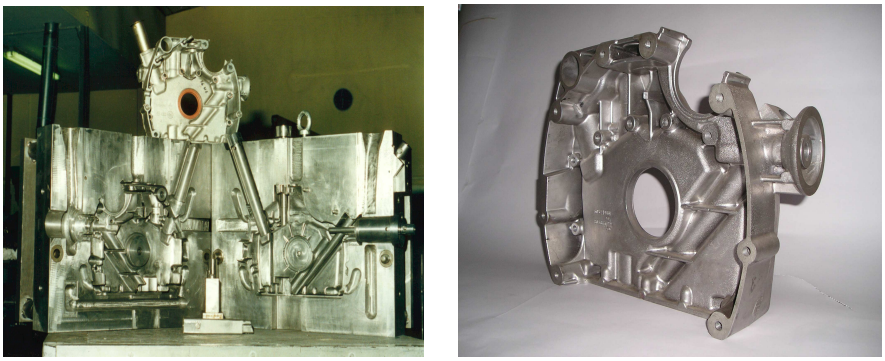

Fig. 3. Steel mould used in a gravity die–casting process and the corresponding aluminium casting part.

Generally, only a tetrahedral FE mesh can be generated. The small thickness of many parts, especially in the case of either low–pressure or high–pressure die–casting processes, is a strong constraint when meshing. Very few elements are placed within the thickness of the casting part, posing difficulties

for the numerical description of temperature gradients as well as the evolution of the thermal contraction or the stress field.

The artificial stiffening due to a very coarse mesh discretisation may be the major difficulty in achieving the accuracy needed. Figure 4 shows the original CAD geometry and the FE mesh used for a High Pressure Die–Casting (HPDC) analysis. The mesh generated, including mould and filling system, is about one million linear elements, which is the current practical limit in a standard PC platform. However, just one linear element is placed in the thickness of the part.

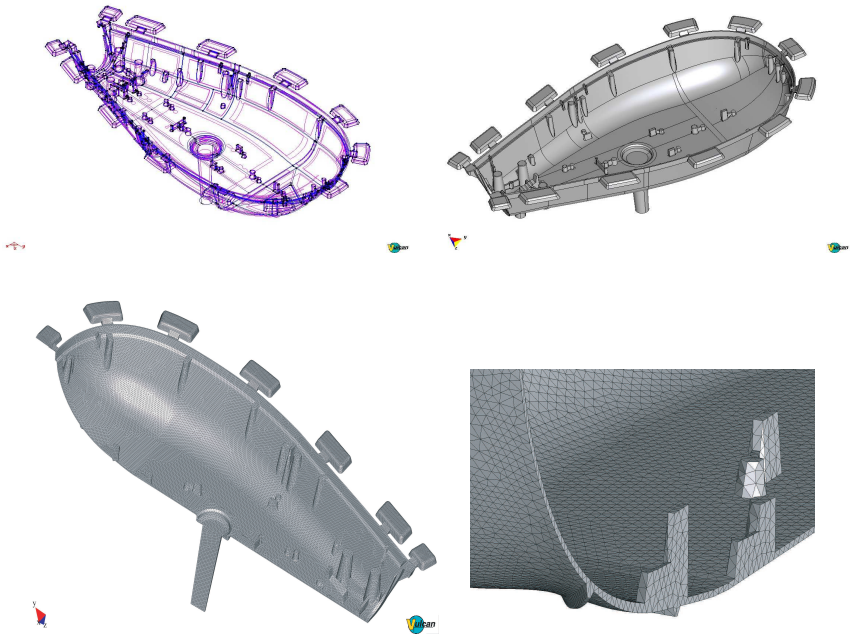

Fig. 4. HP Die–casting process: CAD geometry and FE mesh generated

The artificial stiffening of the discrete model induced by a coarse mesh is increased by the element technology used to respect the volumetric incompressibility constraints as introduced in the previous section. Mechanical contact algorithms in particular suffer such numerical stiffening. Therefore, a very robust contact algorithm must be used to prevent spurious penetrations and numerical locking of the solution.

4 Time Integration Strategy

Another important consideration comes from the fact that an implicit time integration algorithm is usually adopted for the solution of casting simulations. Solidification and the following cooling process can take hours and even days. Explicit formulations, usually adopted in sheet metal forming and forging processes, cannot be used for casting analysis. The use of very small time–steps is the main characteristic of an explicit formulation, leading to a linearisation of the problem in which a very small number of new contact reactions is generated in each time step. In contrast, an implicit algorithm allows for the use of large time–steps but increases their non–linearity. Solution strategies for highly non–linear problems must be chosen e.g. the Newton–Raphson method, linked to a line–search strategy, among others.

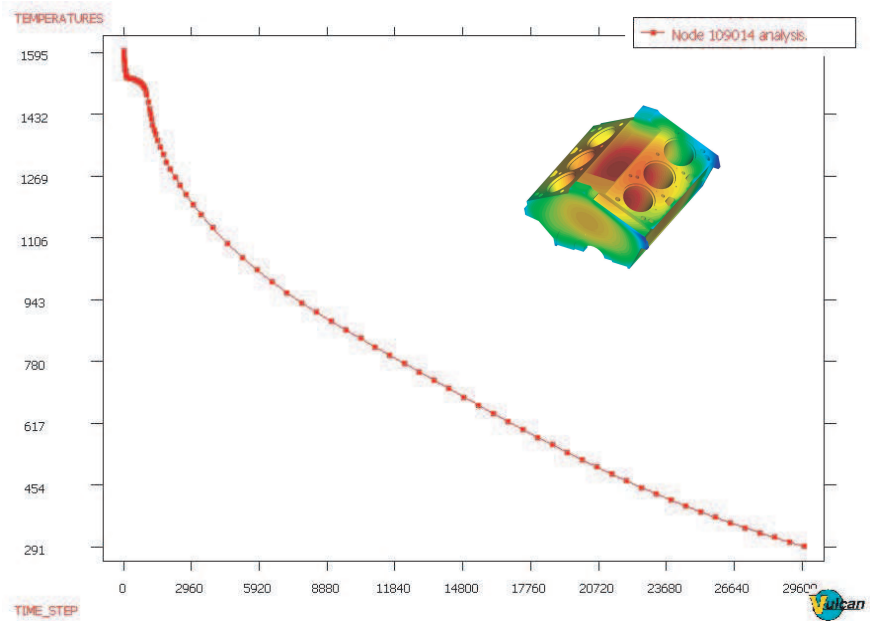

Fig. 5. Virtual thermo–couple in the casting centre

Figure 5 shows the temperature evolution at the centre of the casting. Each point on the curve represents the result of a time–step of the analysis. It is possible to observe how the time–increment during most of the simulation is of order of 1,000 [s]. Such time–stepping completes the solution of the simulation in less than 100 steps.

Additionally, it is important to observe that all the potential contact surfaces are active at the beginning of the casting simulation. Melted metal is in

contact with the mould. During solidification, the shrinkage of the material due to the phase change as well as subsequent contraction occurring during the cooling phase produces a loss of contact constraints. An open air–gap is formed up to the limit case in which the casting part could move. This is a serious problem when a quasi–static analysis is carried out.

A solution is difficult to achieve even if a dynamic algorithm is used. In practice, the very large time steps adopted to follow the temperature evolution reduce or even remove the stabilisation effect due to the inertia term. A possible solution involves the direct constraining of the movement of the casting, and the most natural possibility consists of fixing the nodes at the in–gate.

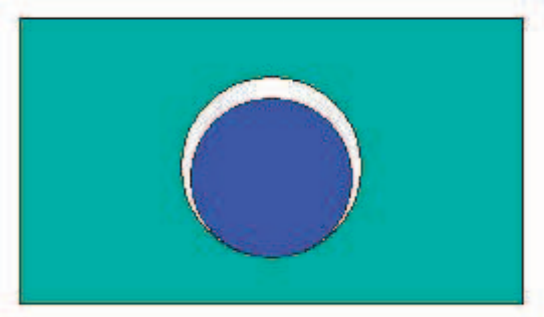

Fig. 6. Casting shrinkage generates loss of contact constraining.

Figure 6 shows a possible contact benchmark test to prove the problem of the loss of constraining when shrinkage occurs. In this case, the in–gate is not defined, so the location of possible prescription is not straightforward and solving this apparently easy problem is not trivial.

5 Discretisation of the Contact Surface

The discretisation of the contact surface is another problem induced by the FE mesh. Surface curvature results in a non–smooth surface definition leading to a non–smooth contact reaction field. The direction of the normal vector at each node of the surface is not univocally defined: there are different possibilities depending on the algorithm selected. All of these possibilities should converge on refining the mesh but if this is not possible (i.e. a large industrial analysis) the mesh choice can seriously affect the final result. Figure 7 shows

three different choices for the normal vector at the corner, which will define the direction of the normal contact reaction when a non–smooth surface is considered.

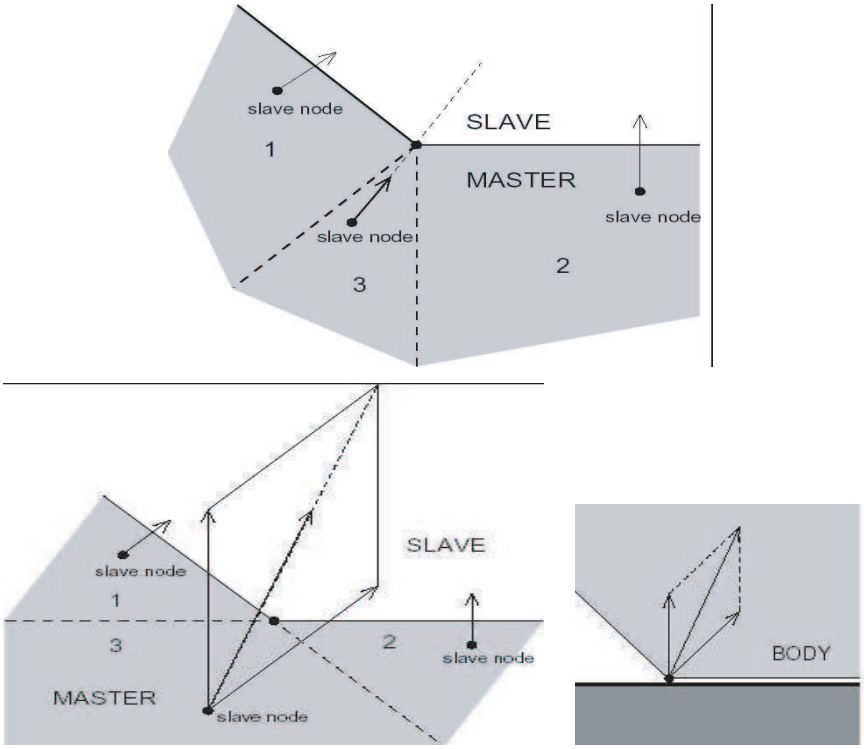

Fig. 7. Definition of the normal vector: a) Slave–master formulation; b) node–to–node formulation; c) contact with a rigid surface.

6 Thermo–Mechanical Contact Algorithms

In a large number of problems, it is necessary to take into account the thermo–mechanical interaction among different bodies in a numerical simulation. High precision in the simulation of contact behaviour is not always required, because the main emphasis can be the overall performance of the structure, as for military impact and crash–worthiness analyses. On the other hand, forming processes such as hot–forging, sheet metal forming or casting analysis demand an appropriate description of the mechanical constraint at the contacting surfaces.

Focusing on foundry processes, it is an extremely important to take into account the numerical simulation of the mechanical interaction among casting

tools (such as part, mould, cores, etc...). Both the solidification and following cooling processes as well as de–moulding phase in a casting analysis is a fully coupled problem where the temperature evolution defines the mechanical behaviour and the mechanical interaction at the contact interfaces affects the heat flux which drives both the temperature and solidification evolution. If we examine the definition of heat conduction and heat convection laws, the importance of an accurate definition of the contact pressure as well as the prediction of the open air–gaps between casting part and mould surfaces is clear. The relationship between heat transfer coefficients and open air–gap has been experimentally proven Hallam, C.P. et al. [2000], Ransing, R.S. and Lewis, R.W. [1998], especially in case of low–pressure but also in high–pressure die–casting processes, which use permanent moulds. Therefore, a truthful prediction of the contact pressure and open air–gap widths is essential to produce a reliable casting model.

In the literature it is possible to find many different algorithms to study the mechanical contact between deformable bodies, Wriggers, P. [2002]. The solution of a contact problem involves, first, the identification of the contact zone on the boundary and, second, the definition of an appropriate condition to prevent penetration. In a solidification process the contraction of the poured material is in of order of 3–5% of the original volume and no other movements are allowed. It is thus possible to assume a small displacement contact algorithm. This hypothesis reduces the cost associated to the so–called *closest–point–projection* procedure, which is commonly used when large slip can occur, and it is necessary to find the projection of any node of one surface (slave surface) on the other surface (master surface) currently in contact Laursen, T.A. and Simo, J.C. [1993]. A simpler node–to–node or face–to–face contact algorithm can be assumed without loss of accuracy.

Once the contact zone is identified and discretised, two different typologies of contact algorithms can be applied to prevent the penetration, thereby establishing the contact constraints. On one side, the so–called **soft contact**. It is possible to include all algorithms based on penalisation techniques, such as the Penalty method (P–method) or the *augmented Lagrangian* algorithm (AL–method), among others Agelet de Saracibar, C. [1998], Ju, J.W. and Taylor, R.L. [1998], Laursen, T.A. and Simo, J.C. [1993], within category . The contact constraint is relaxed by introducing a penalty parameter, which controls penetration at the contact interfaces. The original contact constraint is transformed into the generation of contact elements, whose stiffness depends on the value of the penalty parameter selected.

A possible alternative is the **hard contact** formulation. Mechanical contact problem is solved by computing the contact reactions, which totally prevent the penetration at the contact interface: the so–called *Lagrange multipliers*.

7 SOFT Contact Algorithms

Each contact algorithm presents advantages and disadvantages, and its use depends on the specific analysis considered. *Softcontact* technology (P– or AL–method, among others) is very flexible, covering a wide range of applications. However, it depends on an a priori definition of the penalty parameter. On the one hand, these contact algorithms fit very well within the Finite Element (FE) framework (contact element are generated when penetration of the two contacting surfaces is detected). On the other, the choice of the right penalty parameter can be very difficult, Wriggers, P. [2002].

The case in which the stiffness of the contacting bodies differs greatly is very problematic, as for example the solidification analysis (melted material has a very low stiffness compared to the mould). Additionally, the stiffness of the casting changes during the entire process in response to the evolution of the temperature field. This temperature field is obviously non–uniform, leading to a non–uniform stiffness of the contacting bodies so that the choice of the right penalty parameter can turn into a nightmare for any software user, Nour–Omid, B. and Wriggers, P. [1987].

Depending on the analysis to be performed, two alternatives are possible:

- *Node–to–node* contact algorithm. This algorithm is suitable only for small displacement analysis. The contacting zone is known a priori: for each node of one surface there exists the corresponding node on the other surface, eliminating the need for expensive search techniques.
- *Node–to–face* contact algorithm based on *slave–master formulation*. Suitable for either small or large slip analysis. A searching algorithm is required to identify the projection of each slave node onto the master surface (i.e. closest point projection algorithm).

In a casting solidification analysis, the easier small displacement formulation can be adopted without losing accuracy. Therefore, coincident surface meshes are generated such that the location of the boundary nodes of the mould, $\mathbf{X}^{(M)}$, here referred to as master nodes, match the location of the casting nodes, $\mathbf{X}^{(S)}$, referred to as slave nodes. A great advantage of this strategy is that neither spurious initial penetrations nor fictitious open–gaps are allowed at the beginning of the simulation.

The following step consists of introducing a constraint condition for any pair of nodes (slave–master pair) in which a penetration is detected. In the following section, the most common methods of tackling such constraining are presented.

7.1 Penalty Method

The most common approach to facing a contact problem within the soft–contact algorithms is the P–method, Agelet de Saracibar, C. [1998], Laursen,

T.A. and Simo, J.C. [1993]. The contribution due to the contact interaction is obtained introducing the following functional:

$$\Pi_c = \frac{1}{2}\int_{\Gamma_c} \varepsilon g_n^2 dS$$

where ε is the penalty parameter and g_n is the normal penetration (gap) defined as:

$$g_n = \mathbf{n}^T \cdot \left[\left(\mathbf{X}^{(M)} + \mathbf{u}^{(M)}\right) - \left(\mathbf{X}^{S} + \mathbf{u}^{(S)}\right)\right] = u_n^{(M)} - u_n^{(S)}$$

where $\mathbf{n}$ is the external normal to the master surface at the master node and $\mathbf{u}^{(S)}$ and $\mathbf{u}^{(M)}$ are the nodal displacements of slave and master nodes, respectively. The first variation Π_c results in:

$$\delta\Pi_c = \int_{\Gamma_c} t_n \delta g_n dS$$

where $t_n = \varepsilon\ g_n$ is the normal pressure at the contact interface restricted by the Kuhn–Tucker conditions:

$$t_n \geq 0 \quad \text{if} \quad g_n = 0$$

$$t_n = 0 \quad \text{if} \quad g_n \geq 0$$

The matrix equation for a nodal pair can be written as, Wriggers, P. [2002], Wriggers, P. and Simo, J.C. [1985]:

$$S \cdot \begin{bmatrix} \varepsilon & -\varepsilon \\ -\varepsilon & \varepsilon \end{bmatrix} \begin{Bmatrix} \delta u_n^{(S)} \\ \delta u_n^{(M)} \end{Bmatrix} = S \cdot \begin{Bmatrix} -t_n \\ t_n \end{Bmatrix}$$

where S is the contact area for the current slave–master pair. Referring to the global axes, the above equation transforms into:

$$\varepsilon S \cdot \begin{bmatrix} (\mathbf{n}\otimes\mathbf{n}) & -(\mathbf{n}\otimes\mathbf{n}) \\ -(\mathbf{n}\otimes\mathbf{n}) & (\mathbf{n}\otimes\mathbf{n}) \end{bmatrix} \begin{Bmatrix} \delta\mathbf{u}^{(S)} \\ \delta\mathbf{u}^{(M)} \end{Bmatrix} = S \cdot t_n \begin{Bmatrix} -\mathbf{n} \\ \mathbf{n} \end{Bmatrix}$$

In a Penalty approach, the final penetration is not zero and it depends on the value of the penalty parameter selected. This is an important problem in the case of casting analysis because it is really difficult to select the appropriate penalty value. In practice, this value is usually taken as a function of the stiffness and element sizes of the contacting bodies. It is also a fact that, during both the solidification and the cooling processes, casting stiffness is changing drastically making it difficult to choose the penalty. Some authors propose a temperature–dependent parameter according to the temperature evolution at the casting interface, Jaouen, O. and Bellet, M. [1998]. Even if the results improve, the use of fairly large values of the penalty parameter to prevent the penetration of one boundary to the other is still problematic.

It must also be observed that the use of iterative solvers, such as a conjugate gradient or GMRES iterative solvers is a very attractive alternative for the solution of large–scale industrial problems. The number of iterations necessary to achieve the solution is a function of the condition number of the matrix of the system. By adding the contact contributions to the assembled matrix (which depend on the value of the penalty parameter used), the number of iterations required by the solver to converge increases, and as a direct consequence, the total CPU time. High values of the penalty parameter lead to a matrix ill–conditioning up to the limit case of solver locking.

7.2 Augmented Lagrangian Method

An alternative to reduce matrix ill–conditioning, without losing quality of results, is the AL–method, Agelet de Saracibar, C. [1998]. The strategy consists of a recursive improvement of the contact pressure through an augmentation loop, which allows the use of lower penalty parameters to achieve similar or even better results.

The algorithm can be stated as:

$$\begin{bmatrix} k & -k \\ -k & k \end{bmatrix} \left\{ \begin{array}{c} du_n^{(s)} \\ du_n^{(m)} \end{array} \right\} = \left\{ \begin{array}{c} -\lambda^i - t_n \\ \lambda^i + t_n \end{array} \right\}$$

where the update of the Lagrange multiplier λ^i (contact pressure) is computed as:

$$\lambda^{i+1} = \lambda^i + t_n$$

Such an update can be computed either after each Newton–Raphson iteration or in an added iteration loop after converging. In either case, loss of quadratic convergence and the high cost induced by the new augmentation–loop are drawbacks of the method.

7.3 Block Iterative Method

As a third alternative, the authors propose, a block–iterative solution. The basic idea consists of using a P–method together with the decomposition of the final system of equations into casting, mould and contact equations, such as:

$$\begin{bmatrix} \mathbf{A}_{cast} & \mathbf{0} & \mathbf{A}_{c,cast} \\ \mathbf{0} & \mathbf{A}_{mold} & \mathbf{A}_{c,mold} \\ \mathbf{A}_{c,cast} & \mathbf{A}_{c,mold} & \mathbf{A}_c \end{bmatrix} \left\{ \begin{array}{c} d\mathbf{u}_{cast} \\ d\mathbf{u}_{mold} \\ d\mathbf{u}_c \end{array} \right\} = \left\{ \begin{array}{c} \mathbf{r}_{cast} \\ \mathbf{r}_{mold} \\ \mathbf{r}_c \end{array} \right\}$$

where the contact equations are those associated with the nodes at the contact interface. As a result, an arrow shaped system of equations is obtained. An iterative solution of such a system is proposed in the form:

$$\mathbf{A}_{cast}\ d\mathbf{u}_{cast}^{i+1} = \mathbf{r}_{cast} - \mathbf{A}_{c,cast}\ d\mathbf{u}_{c}^{i}$$

$$\mathbf{A}_{mold}\ d\mathbf{u}_{mold}^{i+1} = \mathbf{r}_{mold} - \mathbf{A}_{c,mold}\ d\mathbf{u}_{c}^{i}$$

$$\mathbf{A}_{c}\ d\mathbf{u}_{c}^{i+1} = \mathbf{r}_{c} - \mathbf{A}_{c,cast}\ d\mathbf{u}_{cast}^{i+1} - \mathbf{A}_{c,mold}\ d\mathbf{u}_{mold}^{i+1}$$

where index i stands for the iteration counter within the block–iterative solution.

The advantages of this procedure are manifold: first, the local matrices that solve each of the sub–problems generated are much better conditioned, leading to a much better performance of any iterative solver chosen. Second, the partial problems to be solved are smaller and thus faster to solve. Finally, the proposed structure can be parallelized easily, so that casting and mould can be assembled and solved using different processors. The only information to be transferred is the vector of nodal unknowns. We must point out a drawback of the method: the number of iterations required by the block–iterative method proposed depends on the penalty parameter used. Therefore, even if better control is achieved on the global solution, the performance still depends on the conditioning of the original matrix.

In the following Tables we can see the typical Newton–Raphson convergence evolution for the three methods described.

The AL–method shows a faster convergence evolution than the standard P–method. However, the total number of iterations necessary to solve the time–step is higher requiring longer CPU time. If we look at the block–iterative method, it is possible to judge the good performance of the Newton–Raphson convergence even if the total number of iterations is still high.

It must be pointed out that when simulating a huge industrial model the loss of convergence due to the use of an unsuitable penalty parameter is frustrating. The simulation must be started over without any additional guaranty and with much time lost.

The block–iterative procedure gives a solution even if the iterative loop is not fully converged. This solution, probably violates the non–penetration constraint imposed by the mechanical contact, but it allows the solution of the following time–step without stopping the full simulation process due to a loss of convergence of the global analysis.

8 HARD Contact Algorithms

Hard–contact technology solves the contact problem by adding constraints to the weak form of the balance of momentum equation. This is achieved by introducing the following potential to the mechanical problem:

$$\Pi_c = \int_{\Gamma_c} \lambda_n g_n dS$$

Penalty Method	Convergence Ratio	**Augmented Lagrangian**	Convergence Ratio	**Block-Iterative Method**	Convergence Ratio
IT.=1	1.000000E+3	IT.=1	1.000000E+3	IT.=1	1.00000E+3
IT.=2	2.245836E+2	IT.=2	8.957635E+2	IT.=2	6.84654E+1
IT.=3	2.093789E+2	IT.=3	7.846474E+0	IT.=3	8.57626E-2
IT.=4	7.473996E+1	IT.=4	6.735237E-3	*BLOCK-ITER*	
IT.=5	5.873453E+1	*NEW AUGM*		IT.=4	2.97468E+1
IT.=6	9.986438E+0	IT.=5	5.734238E+1	IT.=5	4.845342E-2
IT.=7	3.762686E-2	IT.=6	6.723579E-3	*BLOCK-BLOCK*	
IT.=8	2.125986E-4	*NEW AUGM*		IT.=6	4.734127E-3
		IT.=7	3.946447E-3		

Table 1. Typical convergence performance obtained using the standard P–method, the AL–method and the proposed block–iterative method

where λ_n are the contact reactions (Lagrange multipliers), a new set of unknowns to be added to the standard nodal variables of the coupled thermo–mechanical problem (displacements, pressures, temperatures,...). The variation of Π_c leads to the contact (constraining) term to be added to the weak form of the balance of momentum equation:

$$\delta\Pi_c = \int_{\Gamma_c} (\lambda_n \delta g_n + g_n \delta\lambda_n)\, dS$$

The first term of the above integral corresponds to the variation of the virtual work done by the contact pressure λ_n, along the variation of the gap function. The second term describes the enforcement of the constraints. The associated matrix format can be written as:

$$S \cdot \begin{bmatrix} 0 & 0 & \mathbf{n} \\ 0 & 0 & -\mathbf{n} \\ \mathbf{n} & -\mathbf{n} & 0 \end{bmatrix} \left\{ \begin{array}{c} \delta\mathbf{u}^{(S)} \\ \delta\mathbf{u}^{(M)} \\ \delta\lambda_n \end{array} \right\} = S \cdot \left\{ \begin{array}{c} \mathbf{n} \cdot \lambda_n \\ -\mathbf{n} \cdot \lambda_n \\ g_n \end{array} \right\}$$

where S is the contact area associated with the slave–master pair.

Two remarks are relevant from the above equations: first, the number of unknowns increases as compared to the system without constraining. A new unknown is added for each slave–master pair. This could be inconvenient in terms of the CPU time required for the solution: in the case of a thin–walled part, the number of nodes on the surface is of the same order as in the volume. Second, the system of linear algebraic equations is no longer positive–definite and in fact it has a zero diagonal element for each contact pair. An adhoc solver is required to consider zero–values in the diagonal of the system of equations.

Observe that the contribution to the contact reaction of each node of the surface is evident in the case of coincident surface meshes (this is the case for casting processes), while it is not straightforward when non–coincident meshes are adopted (both forging and sheet–metal forming process simulations need a large slip strategy).

The clear advantage of the hard contact formulation is the accuracy of the final solution in terms of both contact reactions and satisfaction of the contact constraining (they do not depend on a penalty parameter).

Finally, it must be pointed out that the simplest version of this algorithm considers just one deformable body (the cast), while the other bodies involved in the simulation (moulds, cores,...) can be assumed to be rigid. Mechanical contact is treated as a local constraint at the boundary. In this case, the lagrange multipliers can be condensed, as for standard fixity conditions in a local system of reference. As a consequence, the CPU time requirement is dramatically reduced.

9 Thermal Contact Model

Accurate knowledge of the interfacial heat transfer coefficient between the solidifying casting and the surrounding mould is essential to produce a realistic solidification model. Hence, a reliable thermal contact model must be considered, including heat conduction, convection as well as radiation laws, Wriggers, P. and Zavarise, G. [1993].

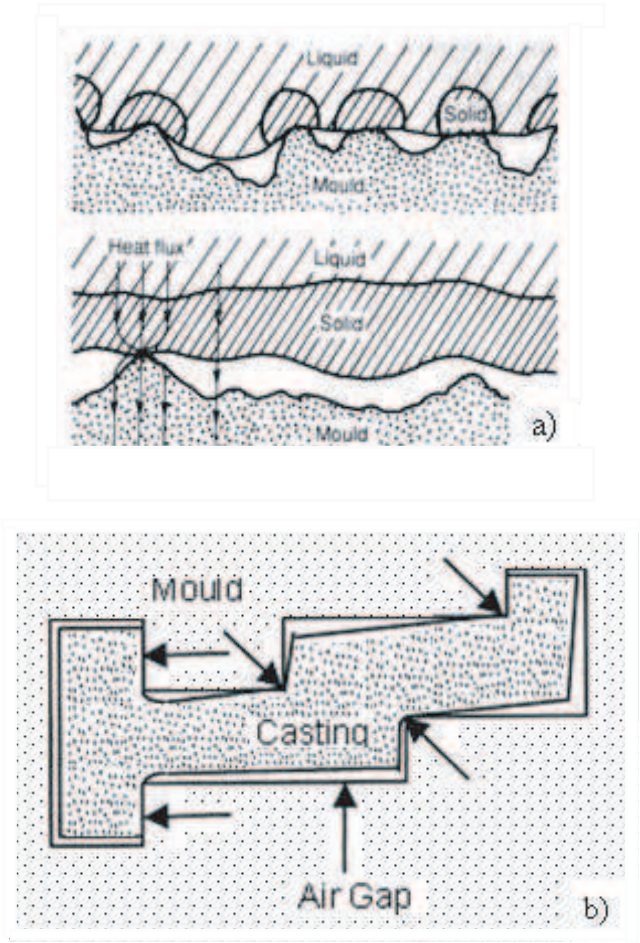

Fig. 8. Thermal contact model. a) The heat conduction coefficient is a function of the effective contact area, which depends on the contact pressure. b) Depending on the casting shrinkage, thermal conduction or thermal convection must be considered.

9.1 Heat Conduction Model

We refer to heat flux by conduction, Q_{cond}, when the casting surface is in contact with the mould surface. In this case, the heat flux is computed as the product of a heat transfer coefficient, h_{cond}, multiplied by the thermal gap, $g_\theta = T_{cast} - T_{mould}$, between the casting and mould surfaces in the form:

$$Q_{cond} = h_{cond}\,(t_n) \cdot (T_{cast} - T_{mould})$$

The heat transfer coefficient can be assumed as a function of the normal contact pressure,t_n, between the two contacting surfaces. The model assumes

a thermal resistance, R_{cond}, due to the air trapped in between the mould and the casting surfaces and induced by the roughness values measured on those surfaces (see Fig. 8). In addition, the thermal resistance due to the mould coating must also be considered, so that the total thermal resistance is computed as:

$$R_{cond} = \frac{R_z}{k_{air}} + \frac{\delta_{coat}}{k_{coat}}$$

where $R_z = 0.5\sqrt{R_{z,cast}^2 + R_{z,mould}^2}$ is the mean peak–to–valley height of the rough surfaces, δ_{coat} is the effective thickness of the coating and k_{air} and k_{coat} are the thermal conductivities of the gas trapped and the coating, respectively.

Moreover, the model assumes that the microscopical interaction between the contacting surfaces (effective contact surface) is proportional to the normal contact pressure. The heat conduction coefficient, h_{cond}, is thus defined using the following expression:

$$h_{cond}\left(t_n\right) = \frac{1}{R_{cond}}\left(\frac{t_n}{H_e}\right)^b$$

where H_e is the Vickers hardness and $0.6 \leq b \leq 1.0$ is a constant exponent, Hallam, C.P. et al. [2000], Ransing, R.S. and Lewis, R.W. [1998].

9.2 Heat Convection Model

Heat convection between two bodies arises when they separate from each other due to the thermal shrinkage effect. Heat convection flux, Q_{conv}, is assumed to be a function of a coefficient, h_{conv}, multiplied by the thermal gap in the form:

$$Q_{conv} = h_{conv}\left(g_n\right) \cdot \left(T_{cast} - T_{mould}\right)$$

It can be verified experimentally that the heat transfer coefficient, h_{conv} depends on the open air–gap, g_n, (the distance between the two surfaces) due to the insulating effect of the gas trapped in the cavity:

$$h_{conv}\left(g_n\right) = \frac{k_{air}}{g_n}$$

However, the above expression must be limited by the value assumed by the heat conduction coefficient, so that:

$$h_{conv} = \max\left(\frac{k_{air}}{g_n}, h_{cond}\right)$$

The model presented above is recommended for permanent mould casting. This is the case of low–pressure and high–pressure die–casting technologies. The high conductivity of the metallic (steel) mould drops when an air gap

is formed due to the shrinkage of the casting material. Air (trapped gas) conductivity is much lower than steel conductivity, and the insulating effect is evident.

Observe that either the contact pressure (used to compute the heat conduction coefficient) or the gap formation can be taken into account only if a coupled thermo–mechanical simulation is performed. Both solidification and cooling evolution are driven by the heat flux exchanged through the boundaries and this heat flux is coupled with the mechanical behaviour. If a purely thermal model is used to compute the solidification evolution, a lack of information must be assumed and a simplified model for the heat flux exchange must be considered.

In this case, both heat conduction and heat convection models can depend only on the temperature field, the only nodal variable computed. Both models reduce to:

$$Q_{conv} = h_{ther} \cdot (T_{cast} - T_{mould})$$

where the heat transfer coefficient, h_{ther}, can be a function of the temperature field. Proposals introduced by different authors assume as driving variables the temperature of the casting surface or the temperature of the mould surface, or even an average (air) temperature field.

In our opinion, the temperature field at the contact surface is not representative of the heat flux behaviour making it very difficult to distinguish between heat conduction and heat convection behaviour. It is easy to observe, experimentally as well as numerically, that the surface temperature of the casting material drops very rapidly when it comes in contact with the mould. Surface skin becomes solid even if casting volume is still mainly liquid. As a result, the temperature field on the surface is not representative of the solidification evolution of the part (thermal shrinkage).

To overcome this problem, we propose a heat transfer coefficient as a function of the percentage of solidified casting material, $h_{ther}\left(F_S\right)$, where F_S takes into account the evolution of the solidification as

$$F_S = \frac{1}{V} \int f_S\left(T\right) dV$$

where $0 \leq f_S\left(T\right) \leq 1$ is the solid fraction function computed at each point of the casting volume. As a result the heat flux is defined as a function of the volumetric contraction of the casting, which is an average open air–gap all around the part. Given this, the heat transfer coefficient is computed as:

$$h_{ther}\left(F_S\right) = F_S \cdot \overline{h}_{conv} + \left(1 - F_S\right) \cdot \overline{h}_{cond}$$

where $\overline{h}_{cond}$ and $\overline{h}_{conv}$ are average values for the heat conduction and heat convection coefficients, respectively.

Finally, observe that a heat convection model should be considered to deal with the thermal flux with the surrounding environment. A similar model

based on the product between a heat transfer coefficient and the thermal gap is used:

$$Q_{conv,env} = h_{env}\left(T_{env}\right) \cdot \left(T_{mould} - T_{env}\right)$$

Note that the heat transfer coefficient depends on the casting temperature in contact with the environment $h_{env}\left(T_{cast}\right)$, assuming that the air convection generated is proportional to the existing thermal gap.

9.3 Heat Radiation Model

Heat radiation flux between two facing bodies is computed using the Stefan–Boltzmann law:

$$Q_{rad} = h_{rad} \cdot \left[\left(T_{cast} + 273.16\right)^4 - \left(T_{mould} + 273.16\right)^4\right]$$

where the heat radiation coefficient, h_{rad} depends on the emissivities of the two bodies, ε_{cast} and ε_{mould}, respectively, and the Stefan's constant, σ_a, as:

$$h_{rad} = \frac{\sigma_a}{\left(1/\varepsilon_c + 1/\varepsilon_m - 1\right)}$$

It must be pointed out that, for casting analysis, the two surfaces are coincident so that the view factors can be ignored.

Finally, when the heat is dissipated through the surrounding environment, the radiation law is expressed in the form:

$$Q_{rad,env} = \sigma_a \varepsilon_{cast} \cdot \left[\left(T_{cast} + 273.16\right)^4 - \left(T_{env} + 273.16\right)^4\right]$$

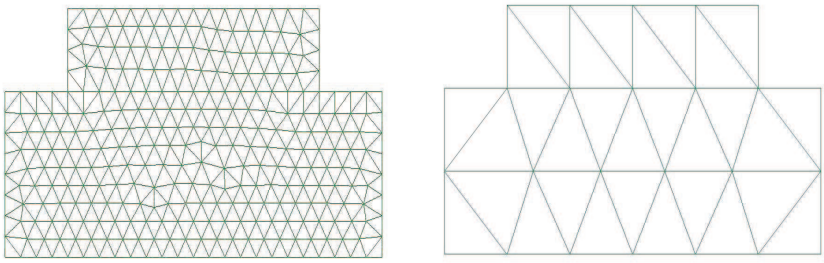

Fig. 9. Contact benchmark. a) Fine mesh; b) Coarse mesh.

10 Numerical Simulations

The formulation presented in previous sections is illustrated here with a number of numerical simulations. The goal is to demonstrate the good performance of the proposed formulation in the framework of infinitesimal strain coupled thermal–plasticity for industrial casting analyses and, in particular, for steel mould casting. Computations are performed with the FE code `VULCAN` developed by the authors at the International Center for Numerical Method in Engineering (CIMNE) in Barcelona, Spain, and commercialised by `QUANTECH-ATZ` VULCAN.

In all the simulations the Newton–Raphson method, combined with a line–search optimisation procedure, is used to solve the non–linear system of equations arising from the spatial and temporal discretisation of the weak form of the governing equations. Convergence of the incremental iterative solution procedure was monitored by requiring a tolerance of 0.1% in the residual based error norm.

10.1 Penalty vs. Augmented Lagrangian Method

This example is intended to show the important role played by the element size. It is easy to understand that the finer the FE mesh, the more deformable the body defined in this mesh, allowing the use of lower values of the penalty parameter to achieve a good solution.

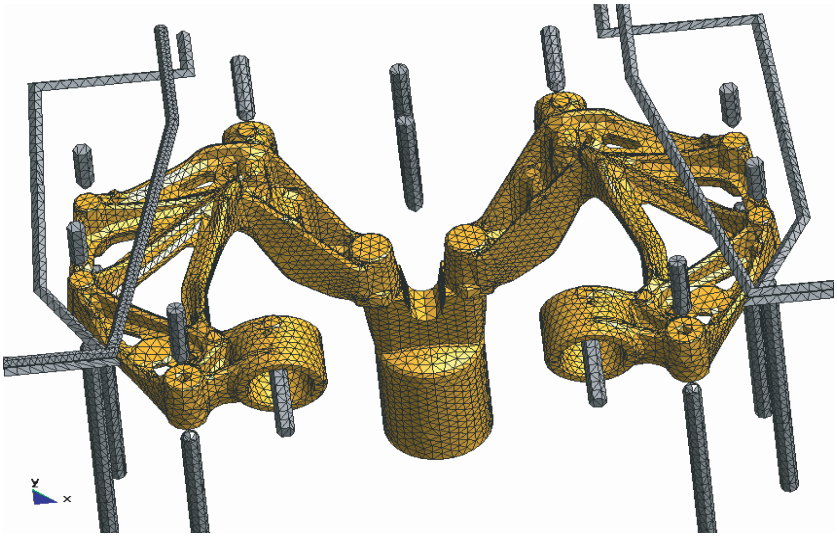

Fig. 10. Automotive part. FE mesh generated for the casting and the cooling system.

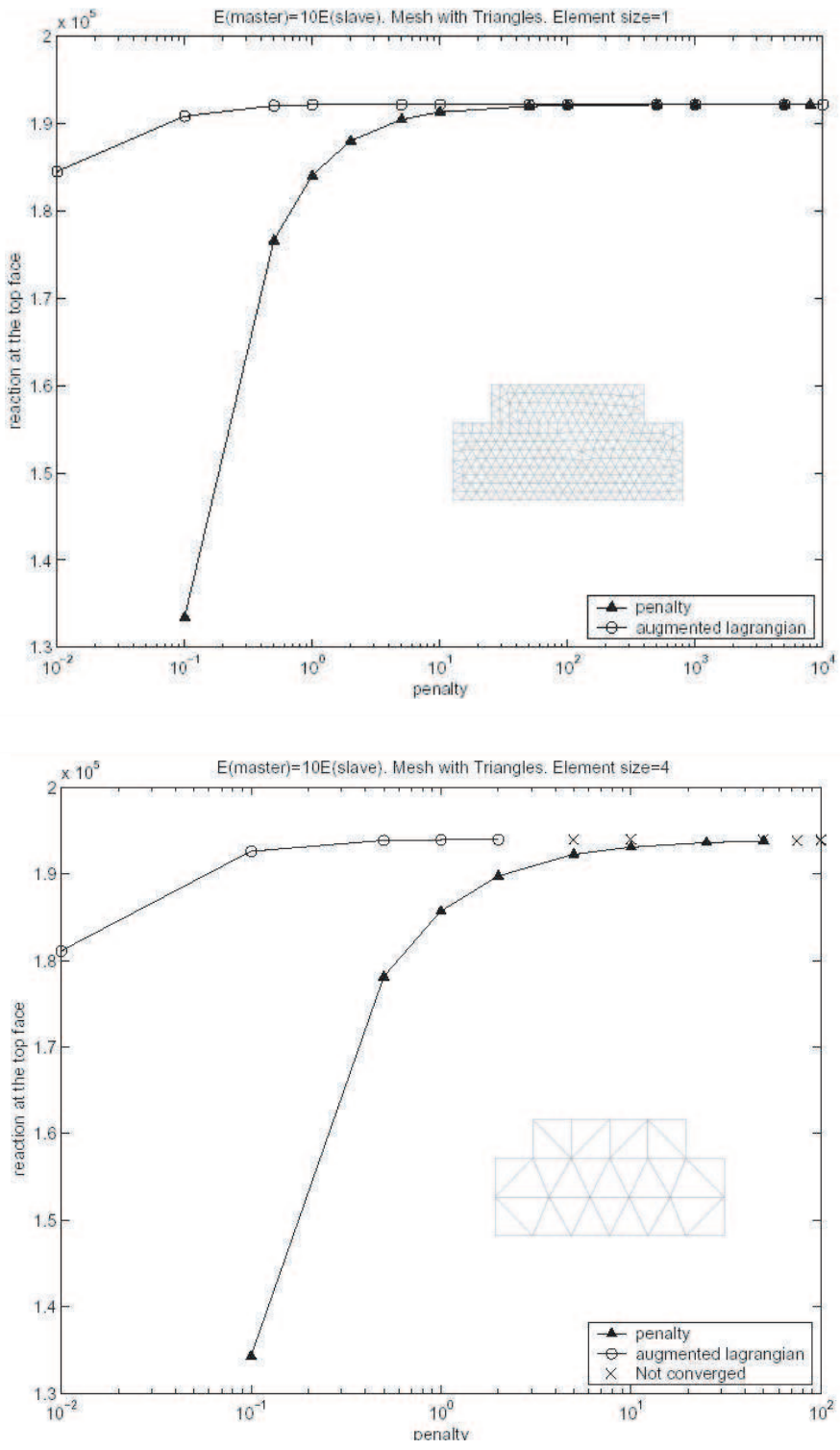

Fig. 11. Contact reaction for both the P– and the AL–methods when increasing the penalty parameter. a) Fine mesh; b) Coarse mesh.

Figure 9 show two different mesh discretisations used to demonstrate the performance of the soft contact formulation. The contact benchmark consists of the upsetting of the upper–block pressed against the base–block. To increase the difficulty, the material stiffness of the base–block is ten times higher compared to the other block.

This benchmark tries to reproduce the situation encounter when solving a real industrial solidification analysis. Figure 10 shows an automotive casting part and the corresponding FE mesh. Half a million elements have been necessary to mesh the full casting system, including cooling channels and mould. Even if the mesh looks good and the total number of elements is close to the computational limit in a standard PC, few elements are placed in the thickness of the part. Hence, mechanical contact presents the same problem shown by the coarse mesh in the contact benchmark.

Figure 11 show the convergence of both the contact reaction and the contact penetration when the penalty parameter is increased. The figure also shows what happens when the coarse mesh is used. It is not possible to achieve the converged solution for high values of the penalty parameter due to locking of the analysis. The convergence to the final solution is slower and often cannot be achieved. In fact, locking of the solution is the main drawback of the penalised methods. Roughly speaking, if a penetration is detected, a contact element is generated. The stiffness of this element in the direction normal to the master surface is set to a very high value compared with the material stiffness of the contacting bodies. To get zero penetration and fully satisfy the impenetrability constraint imposed by the contact condition, an infinite value should be given to the penalty parameter. This is not possible, and it can be demonstrated that the maximum usable value corresponds to the maximum eigenvalue of the final system of equations to be solved. In many cases, this value is not large enough to prevent penetration; and if one tries to increase it, locking of the solution occurs.

The AL–method may be the solution most commonly used to overcome this problem, enabling the use of lower values for the original penalty parameter.

Figures 11 and 12 show how the AL–method has better performance in achieving the converged solution using lower values for the penalty parameter. The Fig. 12, however, clearly presents the weakness of the method in terms of CPU time. The AL–method is two or three times slower than the standard P–method. Hence, even if the choice of a correct penalty parameter is less problematic, the CPU time can increase significantly. According to the experience of the authors, this method is not efficient for large–scale computations.

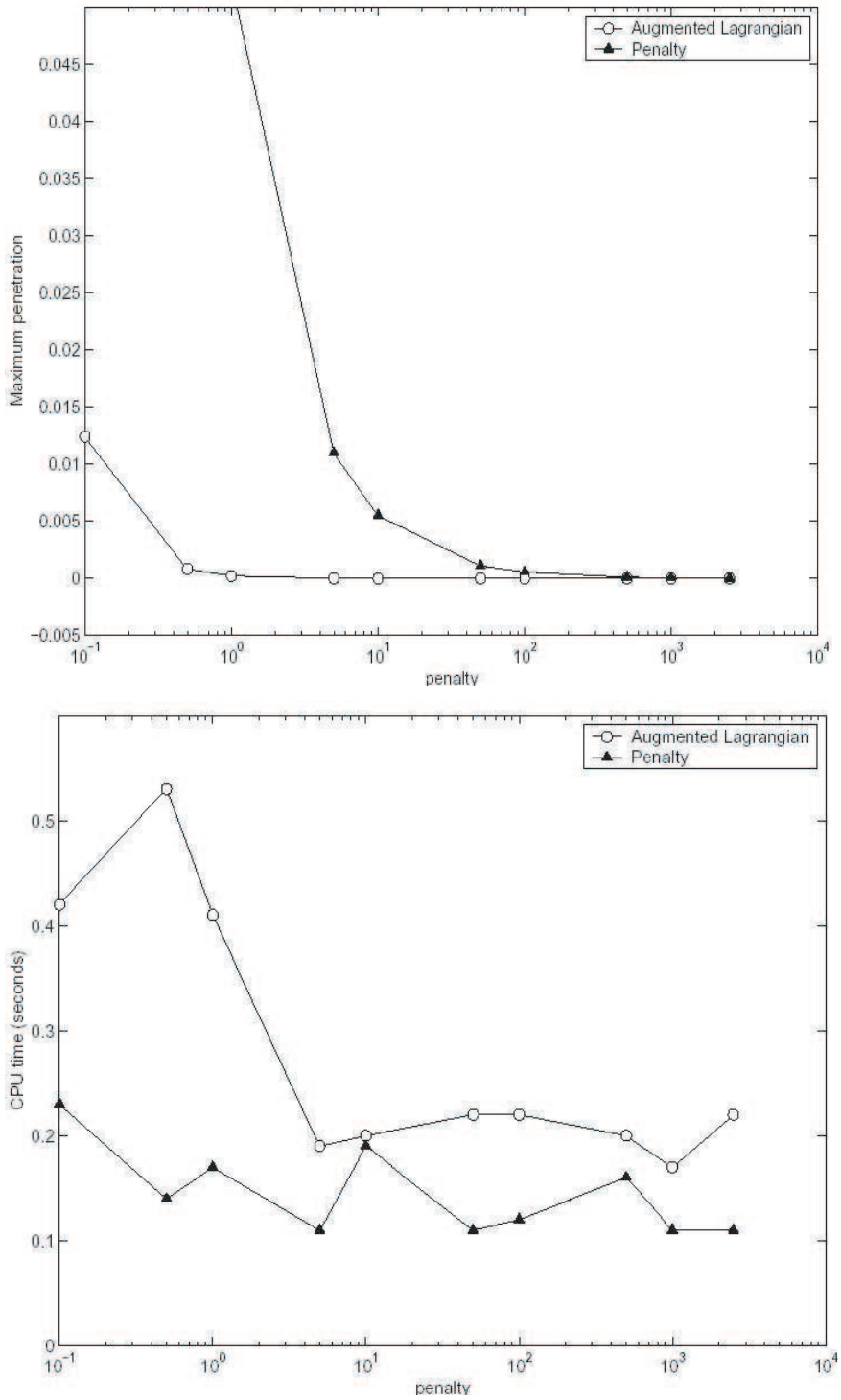

Fig. 12. Contact benchmark: comparison of P– and AL–methods. a) Convergence of the contact penetration to satisfy contact impenetrability constraint when increasing the penalty parameter. b) Cpu–time.

10.2 Thermo–Mechanical Solidification Benchmark

This example is concerned with the solidification process of a cylindrical aluminium specimen in a steel mould. The main goal of this benchmark is to show the accuracy of the fully coupled thermo–mechanical contact model proposed for a solidification analysis. The numerical results have been compared to the experimental values obtained from the literature. The experiment consists of the solidification of commercially pure aluminium into an instrumented mould. Thermocouples have been placed in the mould wall and in the mould cavity.

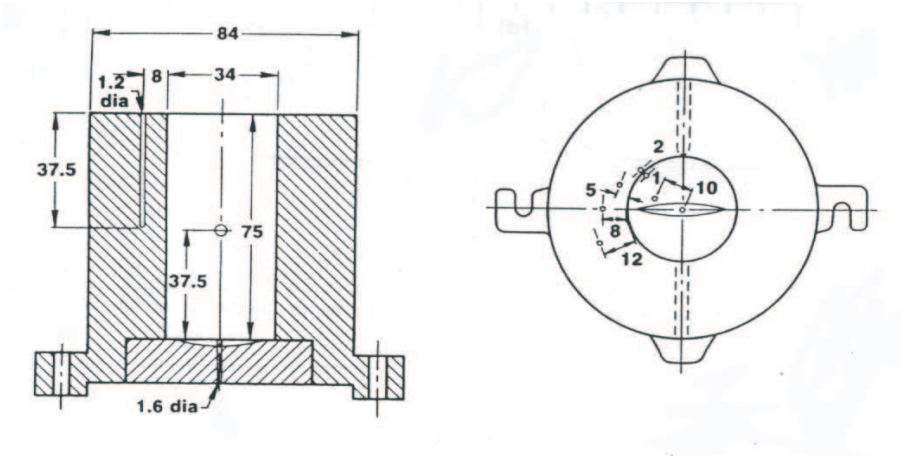

Fig. 13. Cylindrical aluminium solidification test. Geometry of the experimental apparatus and location of both thermocouple and displacement transductors.

The thermocouple locations are shown in Fig. 13. Two quartz rods were inserted into the mould to measure both the displacement of the solidifying cylinder and the mould expansion. The geometry of the problem is shown in Fig. 13. The starting conditions assumed for the numerical simulation consider a completely filled mould with aluminium in liquid state at uniform temperature of 670 [°C] and an initial temperature of the mould set to 200 [°C]. A thermo–elastic constitutive model has been used to simulate the material behaviour of both the aluminium casting and the steel mould. The external surfaces of the mould as well as the upper surface of the casting metal have been assumed to be perfectly insulated. A constant heat transfer coefficient by conduction h_{cond}=2300 [W/m^{2}s] has been assumed as the limit value of the convection–radiation heat flux between the aluminium part and the steel mould as a function of the open air–gap.

Fig. 14. Cylindrical aluminium solidification test. Temperature evolution: (a) 10 [s], (b) 20 [s], (c) 40 [s] and (d) 90 [s]

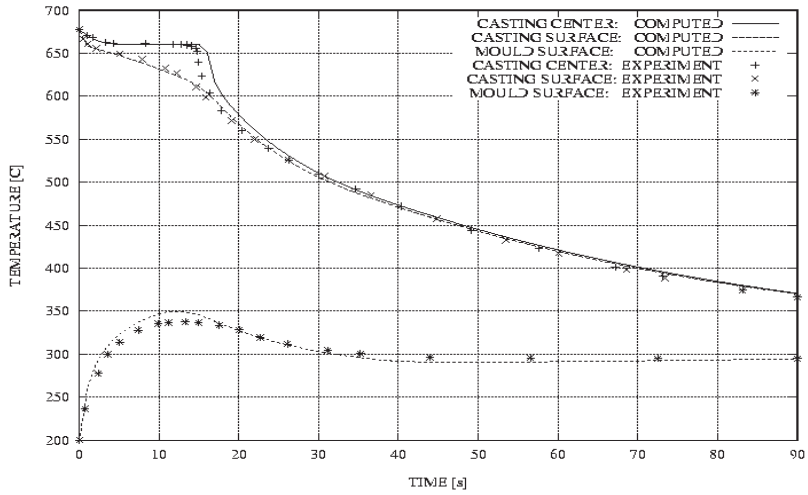

Fig. 15. Comparison of the computed and experimental values of the temperature at the casting centre, casting surface and mould surface, respectively.

Figure 15 compares the temperature evolution at the casting centre, casting surface and mould surface to the experimental data. Figure 16 shows the evolution of the radial displacements for both casting and mould surfaces. The difference between the two curves corresponds to the evolution of the open air–gap. The temperature and air gap evolution predicted by the model compare very well with the experimental results, demonstrating the accuracy of the thermo–mechanical model presented.

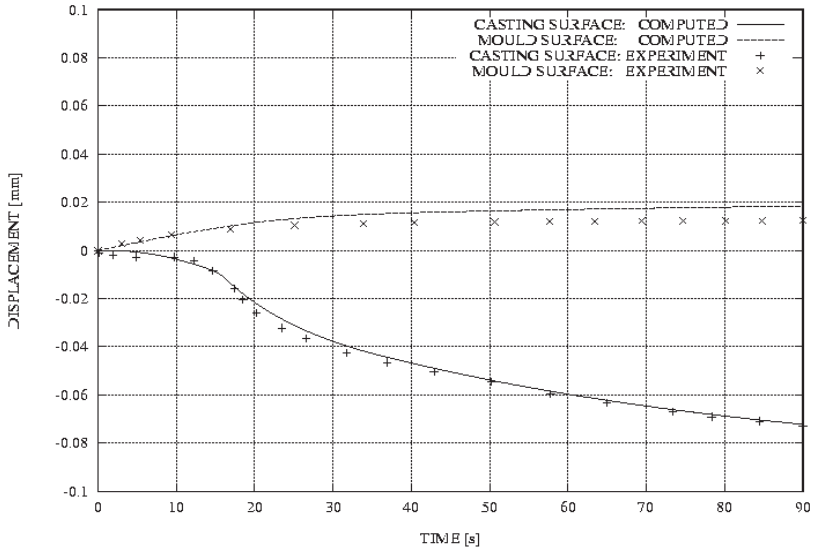

Fig. 16. Comparison of the computed and experimental values of the radial displacement on the casting surface and mould surface, respectively.

10.3 Foundry Simulation of an Automotive Part

The next example is intended to show the results that can be achieved when simulating the solidification process of an automotive component. Figure 17 shows different views of the geometry and FE mesh used for the casting part. The full mesh, including the mould, consists of 240,000 tetrahedral elements. Geometrical and material data were provided by the `TEKSID` Aluminium foundry division. Casting material behaviour has been modelled by the fully coupled thermo–visco–plastic model, while a simpler thermo–elastic model has been assumed to describe the constitutive law for the mould.

Hard contact algorithm has been chosen to deal with the mechanical interaction. Heat radiation, heat conduction and heat convection model as a function of the air–gap resistance due to the casting shrinkage have been taken into account for the simulation.

The initial temperature is 650 [°C] for the casting and 250 [°C] for the mould. The cooling system has been kept at 20 [°C].

Temperature and solid fraction distribution during solidification are shown in both Figs. 18, respectively. Figure 19 shows J2 von Mises deviatoric stress distributions at different sections of the part.

In these figures it is also possible to appreciate the open air–gap between the part and the mould, since this air–gap is responsible for a non–uniform heat flux at the contact interface.

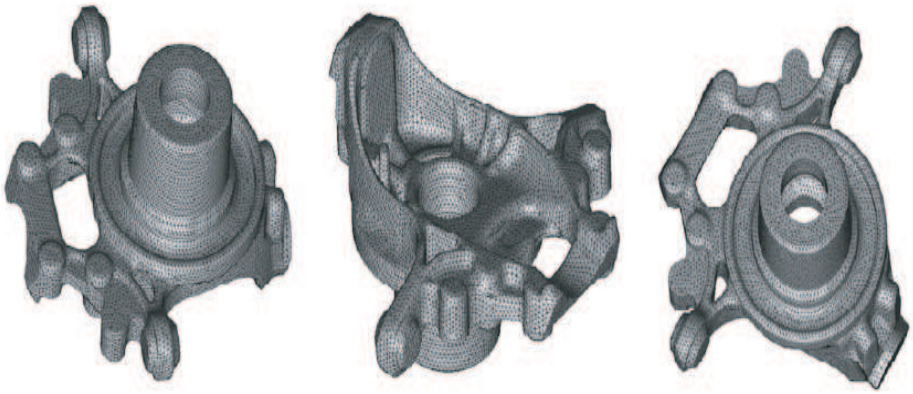

Fig. 17. Different view of the geometry and FE mesh generated for the part studied.

10.4 Foundry Simulation of an Aluminium Motor–block

The final numerical simulation is concerned with the solidification process of an aluminium motor block in a steel mould. Geometrical and material data were provided by the `TEKSID` Aluminium foundry division. Figure 20 shows a view of the FE mesh used for the part and the cooling system. The full mesh, including the mould, consists of 580,000 tetrahedral elements. Aluminium material's behaviour has been modelled by the fully coupled thermo–visco–plastic model, while the steel mould's behaviour has been modelled by a simpler thermo–elastic model. The initial temperature is 700 [°C] for the casting and 300 [°C] for the mould. The cooling system has been kept at 20 [°C]. Temperature evolution and thermal shrinkage during solidification are shown in Fig. 21. Figure 22 shows the temperature, von Mises deviatoric stresses and equivalent plastic strains distributions.

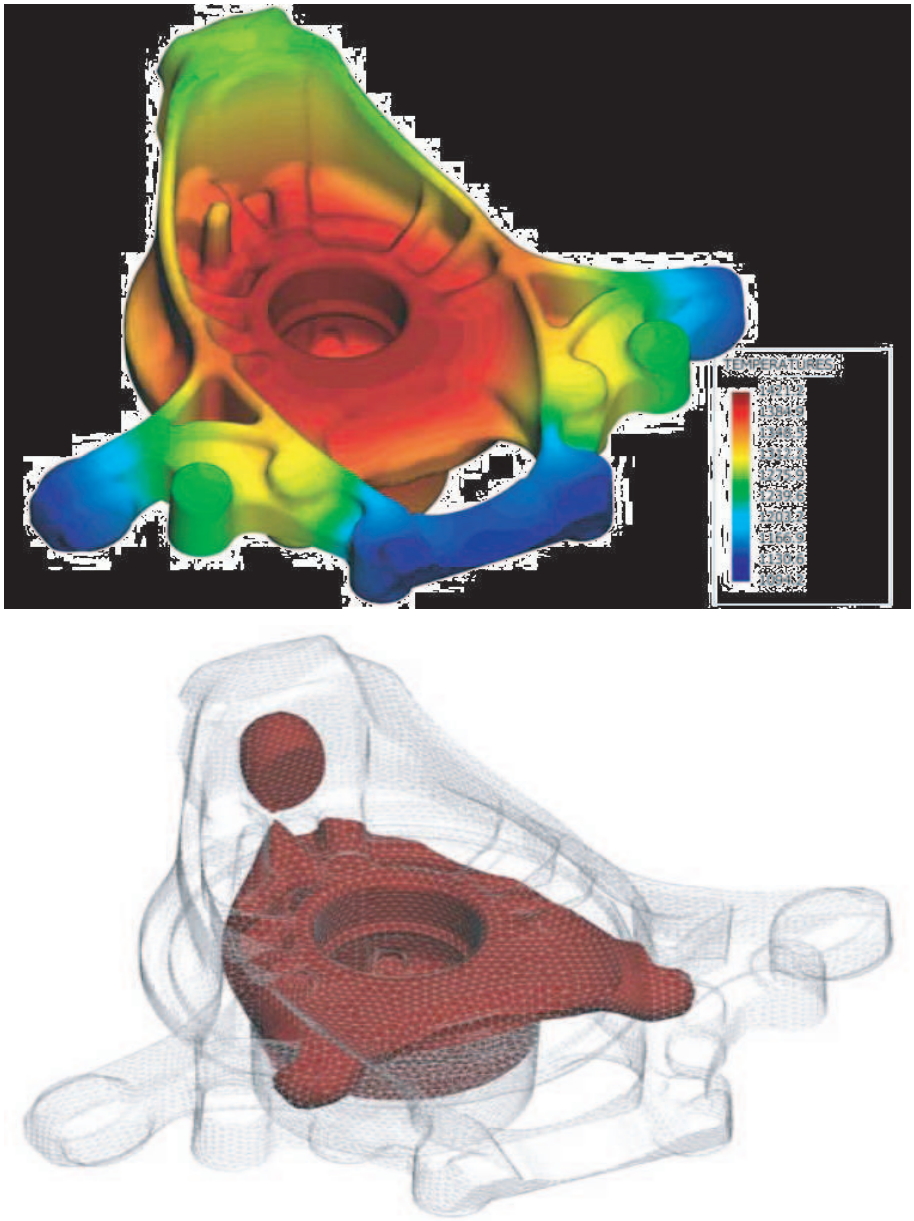

Fig. 18. a) Temperatures distribution at time 1100 [s]. b) Solid fraction contour at time 500 [s].

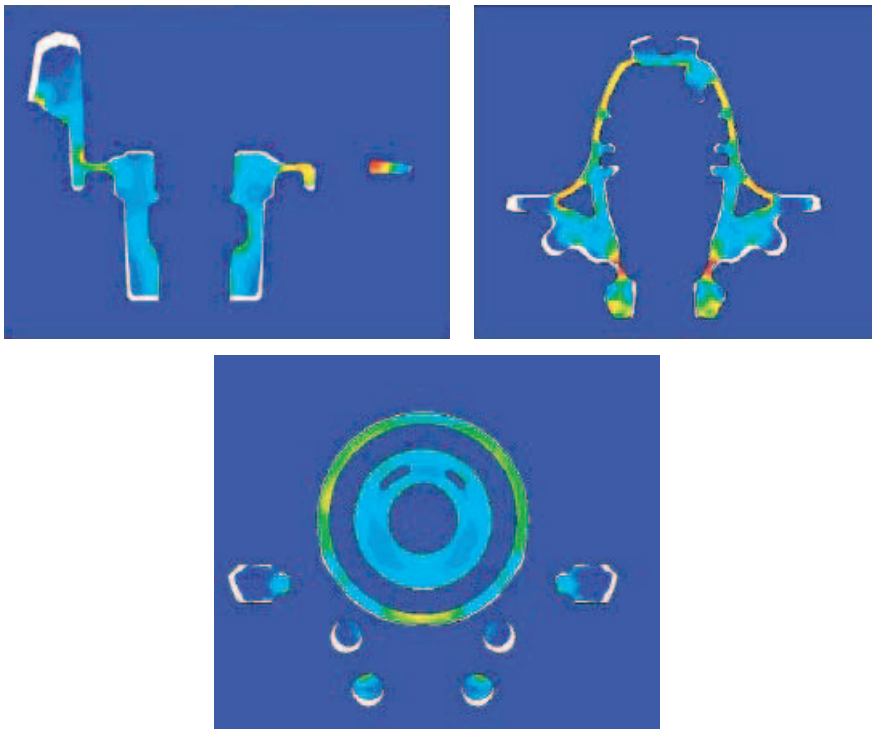

Fig. 19. Contours of J2 von Mises equivalent stress at different sections of the part.

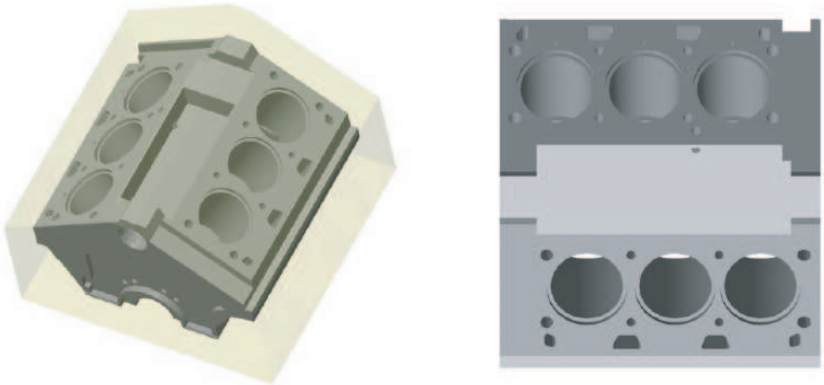

Fig. 20. Geometry of a TEKSID aluminium motor–block casting and mould system.

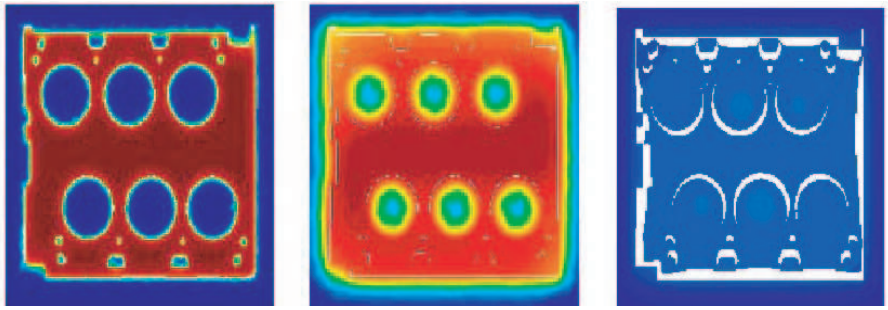

Fig. 21. Temperature and shrinkage evolution (plane xy).

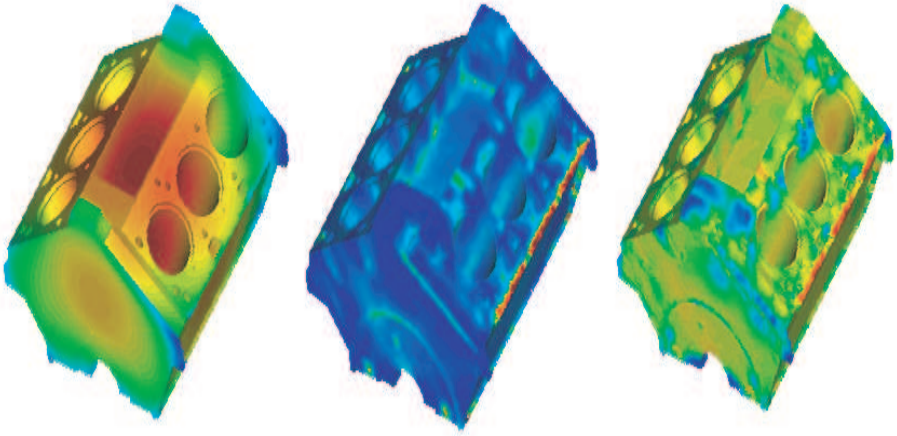

Fig. 22. a) Temperature, b) J2 von Mises and c) plastic strain distributions.

11 Concluding Remarks

A formulation for coupled thermo–mechanical contact problems has been presented. An overview of the different difficulties encountered when solving a thermo–mechanical simulation of a foundry process has been presented. These can be summarized as follows:

In a foundry analysis many casting tools must be represented. Unfortunately, the mesh discretisation that can currently be adopted for computation with a standard PC is usually too coarse. Very few elements can be placed in the thickness of the casting, especially if high–pressure die casting processes

must be simulated. The low capability to capture the high temperature gradients, solidification process and the contact interaction makes it difficult to achieve an accurate simulation. Moreover, the complexity of the CAD geometry obliges the use of tetrahedral elements inducing high numerical stiffening in the solution. This problem is augmented when the incompressibility constraint is enforced, as in the case of liquid–like behaviour or the J2–plasticity constitutive law.

The non–smooth description of the contacting surfaces is another consequence introduced by the mesh discretisation: the vector normal to the surface is non–univocally defined. If the mesh is coarse, the contact reaction field is not uniformly spread.

Furthermore, the use of large time–steps as well as the loss of constraining induced by the shrinkage effect of the casting makes the analysis highly non–linear.

Thermo–mechanical contact plays an extremely important role in a casting analysis, driving the solidification and the subsequent cooling phase. Different phenomenological laws have been presented to account for the heat flux exchanged by the different casting tools involved in the simulation. Among them, a novel definition of the heat transfer coefficient for purely thermal analysis has been proposed. On the other hand, the dependency on mechanical quantities such as the contact pressure or the open air–gap makes the difference when selecting the contact algorithm to represent correctly the mechanical constraining.

This chapter has described different strategies to solve mechanical contact. Within the so–called *soft–contact* algorithms, a novel block–iterative solution has been introduced to enable a better conditioning of each of the sub–problems generated, and thus to achieve better control on the global solution strategy.

However, the radically different stiffness of the contacting bodies as well as the different mesh sizes generally adopted are clear limitations for these methods.

The lagrange multipliers algorithm (*hard–contact*) appears to be the only contact solution, since it is not affected by either the thermo–physical properties or the mesh discretisation of the contacting bodies, especially when coincident surface meshes are assumed. The drawback of this solution is, however, the high number of new unknowns introduced, particularly when the casting geometry presents a very small thickness.

The numerical simulation of real industrial foundry analyses has been performed demonstrating the quality of the results that can be obtained and their dependency on the thermo–mechanical coupling.

Acknowledgements

The support of Martin Solina from QUANTECH ATZ for the numerical simulations performed is gratefully acknowledged.

References

Agelet de Saracibar, C. Numerical analysis of coupled thermo–mechanical frictional contact problems. Computational model and applications. *Archives of Computational Methods in Engineering*, 5:243–301, 1998.

Agelet de Saracibar, C., Cervera, M., and Chiumenti, M. Thermo–mechanical analysis of industrial solidification processes. *Int. J. for Numerical Methods in Engineering*, 46:1575–1591, 1999a.

Agelet de Saracibar, C., Cervera, M., and Chiumenti, M. On the formulation of coupled thermoplastic problems with phase–change. *Int. J. Plasticity*, 15:1–34, 1999b.

Agelet de Saracibar, C., Cervera, M., and Chiumenti, M. On the constitutive modelling of coupled thermomechanical phase change problems. *Int. J. Plasticity*, 17:1565–1622, 2001.

Agelet de Saracibar, C., Cervera, M., Valverde, Q., and Chiumenti, M. A stabilized formulation for elasticity using linear displacement and pressure interpolations. *Computer Methods in Applied Mechanics and Engineering*, 191:5253–5264, 2002a.

Agelet de Saracibar, C., Cervera, M., Valverde, Q., and Chiumenti, M. A Stabilized Formulation for elasticity using linear displacement and pressure interpolations. *Int. J. of Plasticity*, 20:1487–1504, 2002b.

Agelet de Saracibar, C., Cervera, M., Valverde, Q., and Chiumenti, M. Mixed linear simplicial elements for incompressible elasticity and plasticity. *Computer Methods in Applied Mechanics and Engineering*, 192:5249–5263, 2003.

Agelet de Saracibar, C., Cervera, M., Valverde, Q., and Chiumenti, M. On the orthogonal subgrid scale pressure stabilization of finite deformation J2 plasticity. *Computer Methods in Applied Mechanics and Engineering*, 195: 1224–1251, 2006.

Brezzi, F. and Fortin, M. *Mixed and Hybrid Finite Element Methods*. Springer, New York, 1991.

Chiumenti, M., Agelet de Saracibar, C., and Cervera, M. *Constitutive modelling and numerical analysis of thermomechanical phase–change systems*. Monograph M48, CIMNE, Barcelona, 1999.

Codina, R. Stabilization of incompressibility and convection through orthogonal sub–scales in finite element methods. *Computer Methods in Applied Mechanics and Engineering*, 190:1579–1599, 2000.

Hallam, C.P., Griffiths, W.D., and Butler, N.D. Modelling of the interfacial heat transfer between an Al–Si alloy casting and a coated die steel. *Proceedings of IX International Conference on Modelling of Casting, Welding and Advanced Solidification processes*, 2000.

Jaouen, O. and Bellet, M. A numerical mechanical coupling algorithm for deformable bodies: application to part/mold interaction in casting process. *Proceedings of VIII International Conference on Modelling of Casting, Welding and Advanced Solidification processes*, 1998.

Ju, J.W. and Taylor, R.L. A perturbed lagrange formulation for the finite element solution of non–linear frictional contact problems. *J. of Theoretical and Applied Mechanics*, 7:1–14, 1998.

Laursen, T.A. and Simo, J.C. A continuum–based finite element formulation for the implicit solution of multibody, large deformation frictional contact problems. *Int. J. for Numerical Methods in Engineering*, 36:3451–3485, 1993.

Nour–Omid, B. and Wriggers, P. A note on the optimum choice for penalty parameter. *Communications in Applied Numerical Methods*, 3:581–585, 1987.

Ransing, R.S. and Lewis, R.W. Thermo–Elasto–Visco–Plastic Analysis for Determining Air Gap and Interfacial Heat Transfer Coupled with the Lewis–Ransing Correlation for Optimal Feeding Design. *Proceedings of VIII International Conference on Modelling of Casting, Welding and Advanced Solidification processes*, 1998.

VULCAN. *Software for simulation of casting processes.* QUANTECH–ATZ.

Wriggers, P. *Computational Contact Mechanics.* John Wiley and Sons, 2002.

Wriggers, P. and Simo, J.C. A note on tangent stiffness in fully non–linear contact problems. *Communications in Applied Numerical Methods*, 1:199–203, 1985.

Wriggers, P. and Zavarise, G. Thermomechanical contact: a rigorous but simple numerical approach. *Computers & Structures*, 46:47–53, 1993.